

## RADIO OBSERVATIONS OF A LARGE SAMPLE OF LATE M, L AND T DWARFS: THE DISTRIBUTION OF MAGNETIC FIELD STRENGTHS

E. BERGER<sup>1,2,3</sup>*Draft version September 27, 2018*

## ABSTRACT

We present radio observations of a comprehensive sample of 90 dwarf stars and brown dwarfs ranging from spectral type M5 to T8. We detect three radio active sources in addition to the six objects previously detected in quiescence and outburst, leading to an overall detection rate of about 10% for objects later than M7. From the properties of the radio emission we infer magnetic field strengths of  $\sim 10^2$  G in quiescence and nearly 1 kG during flares, while the majority of the non-detected objects have  $B \lesssim 50$  G. Depending on the configuration and size of the magnetic loops, the surface magnetic fields may approach 1 kG even in quiescence, at most a factor of few smaller than in early-M dwarfs. With the larger sample of sources we find continued evidence for (i) a sharp transition around spectral type M7 from a ratio of radio to X-ray luminosity of  $\log(L_R/L_X) \sim -15.5$  to  $\gtrsim -12$ , (ii) increased radio activity with later spectral type, in contrast to H $\alpha$  and X-ray observations, and (iii) an overall drop in the fraction of active sources from about 30% for M dwarfs to about 5% for L dwarfs, fully consistent with H $\alpha$  and X-ray observations. Taken together, these trends suggest that some late-M and L dwarfs are capable of generating 0.1 – 1 kG magnetic fields, but the overall drop in the fraction of such objects is likely accompanied by a change in the structure of the chromospheres and coronae, possibly due to the increasingly neutral atmospheres and/or a transition to a turbulent dynamo. These possibilities can be best addressed through simultaneous radio, X-ray and H $\alpha$  observations, which can trace the effect of magnetic fields on the coronae and chromospheres in a direct, rather than a statistical, manner. Still, a more extended radio survey currently holds the best promise for measuring the magnetic field properties of a large number of dwarf stars.

*Subject headings:* radio continuum:stars — stars:activity — stars:low-mass, brown dwarfs — stars:magnetic fields

## 1. INTRODUCTION

The question of whether and how fully convective low-mass stars and non-hydrogen burning brown dwarfs generate and dissipate magnetic fields has important implications for our understanding of their internal structure and the physical conditions in their atmospheres. Theoretically, the so-called  $\alpha\Omega$  dynamo, which depends on shearing motions at the radiative-convective transition zone, and which is used to explain the origin of the solar magnetic field, cannot operate in fully convective dwarfs. Instead, the magnetic dynamo may increasingly depend on turbulent motions associated with the internal convection itself (Raedler et al. 1990; Durney et al. 1993), but it is not clear if this mechanism can give rise to a large-scale, long-lived magnetic field. Recent magnetohydrodynamic simulations suggest that a large-scale and stable field may in fact be generated, at least for parameters roughly appropriate for an M5 dwarf<sup>4</sup> (Dobler et al. 2006), contrary to earlier indications (Durney et al. 1993). It remains to be seen if the same result holds for the much cooler L and T dwarfs, of which a large fraction lack hydrogen burning as a source of heat.

In addition, it has been argued that even if strong fields are generated, their dissipation may be hampered by the increasingly neutral atmospheres of late-M and L dwarfs (Mohanty et al. 2002). If this is the case, then the suppression of chromospheric and coronal heating will result in decreased emission in the H $\alpha$  emission line, the X-rays, and possibly the radio band, despite the presence of magnetic fields.

Clearly, direct observations which probe the presence, dissipation and properties of the magnetic fields are required to guide and to test these theoretical ideas. Measurements based on Zeeman broadening have been performed for a handful of active early-M dwarfs (up to M4.5), indicating field strengths of a few kG with near unity surface coverage (Saar & Linsky 1985; Johns-Krull & Valenti 1996). Unfortunately, this approach cannot be used effectively for late-M, L and T dwarfs because the required atomic lines are weak in the cool atmospheres of these stars and tend to be blended with molecular features. It has recently been suggested that the field strengths can be measured through a secondary calibration of FeH lines (Reiners & Basri 2006), but this approach is yet to be

<sup>1</sup>Observatories of the Carnegie Institution of Washington, 813 Santa Barbara Street, Pasadena, CA 91101<sup>2</sup>Princeton University Observatory, Peyton Hall, Ivy Lane, Princeton, NJ 08544<sup>3</sup>Hubble Fellow<sup>4</sup>As noted by Dobler et al. (2006), their fiducial model has properties that are typical of M dwarfs, but with an artificially high surface temperature due to numerical limitations.

implemented for any star beyond M4.5.

The presence and dissipation of magnetic fields can be alternatively traced through activity indicators such as H $\alpha$ , X-ray and radio emission. The H $\alpha$  and X-ray emission are secondary indicators since they arise from plasma presumably heated by the dissipation of magnetic fields, through for example magnetic reconnection. In the standard scenario the input of energy drives an outflow of hot plasma into the corona through evaporation of the underlying chromosphere, leading in turn to bremsstrahlung X-ray emission and H $\alpha$  emission (Neupert 1968; Hawley et al. 1995; Guedel et al. 1996). The radio emission, on the other hand, arises from gyroresonance or coherent processes, which trace the presence and properties of magnetic fields directly. Thus, radio observations can be used to infer the field strength of individual objects directly, whereas H $\alpha$  and X-ray emission provide a useful statistical measure and insight into the influence of magnetic fields on the outer layers of dwarf stars.

Observationally, the lack of significant change in the measured level of H $\alpha$  and X-ray activity with the onset of full convection at about spectral type M3, suggests that at least in the early-M dwarfs the putative turbulent or distributed dynamo can operate efficiently. It is also possible that the magnetic field itself acts to reduce the mass at which the transition to fully convective structure takes place (Mullan & MacDonald 2001). However, beyond spectral type M7 there is a precipitous drop in H $\alpha$  and X-ray persistent activity, and only a few percent of the objects exhibit flares (e.g., Reid et al. 1999; Gizis et al. 2000; Rutledge et al. 2000; Liebert et al. 2003; West et al. 2004). Furthermore, unlike in the early-M dwarfs (Rosner et al. 1985; Fleming et al. 1993; Mohanty et al. 2002; Pizzolato et al. 2003), many late-type rapidly rotating dwarfs exhibit little or no discernible activity in these bands (Basri & Marcy 1995; Mohanty & Basri 2003). These patterns are consistent with either a decrease in the generation or dissipation of the magnetic fields, or both.

On the other hand, radio emission has been detected from several late-M and L dwarfs (Berger et al. 2001; Berger 2002; Berger et al. 2005; Burgasser & Putman 2005) suggesting that at least some of these objects are capable of generating and dissipating magnetic fields. Surprisingly, the ratio of radio to X-ray luminosity in the detected objects exceeds by several orders of magnitude the value measured for early M dwarfs and a variety of other stars (including the Sun; Guedel & Benz 1993; Benz & Guedel 1994), and there is no obvious correlation with H $\alpha$  emission. Thus, radio observations present a powerful, and perhaps unique approach for inferring the magnetic field strength of late-type stars and brown dwarfs.

Here we exploit this approach and continue our investigation of radio emission from late-M, L and T dwarfs by expanding the observed sample by about a factor of three (to 90 sources). With this extended sample we find continued evidence for a sharp transition in the ratio of radio to X-ray luminosity at spectral type M7, as well as an increased level of activity with later spectral type. We show, however, that as in the case of H $\alpha$  and X-ray observations,

the fraction of objects producing radio emission drops from about 30% in the M dwarfs to only  $\sim 5\%$  in the L dwarfs. Most importantly, we present for the first time estimates of the magnetic field strength of a large sample of late-M and L dwarfs, and show that for the active sources there is at most a modest drop in the field strength from early-M to early-L dwarfs.

## 2. OBSERVATIONS

We observed a sample of 21 late-M, L and T dwarfs with the Very Large Array (VLA<sup>5</sup>) at 8.46 GHz using the standard continuum mode with  $2 \times 50$  MHz contiguous bands at each frequency. The flux density scale was determined using the standard extragalactic calibrator sources 3C 48 (J0137+331), 3C 147 (J0542+498) and 3C 286 (J1331+305), while the phase was monitored using calibrators located within  $10^\circ$  of the targets sources. The data were reduced and analyzed using the Astronomical Image Processing System. In addition to our observations we obtained and reduced all publicly available observations of late-M, L and T dwarfs from the VLA archive, and collected all measurements published in the literature. This resulted in a total 88 objects ranging from M7 to T8, as well a single M5 dwarf and a single M5.5 dwarf. A summary of all observations and the relevant source properties are given in Table 1 and Figure 1.

For the detected objects we searched for variability (flares) using the following method. We removed all the bright field sources using the AIPS/IMAGR routine to CLEAN the region around each source (with the exception of the target source), and the AIPS/UVSUB routine to subtract the resulting source models from the visibility data. We then plotted the real part of the complex visibilities at the position of the science target as a function of time using the AIPS/UVPLT routine. The subtraction of field sources is necessary since their sidelobes and the change in the shape of the synthesized beam during the observation result in flux variations over the map, which may contaminate any real variability or generate false variability.

## 3. PROPERTIES OF THE RADIO EMISSION

Quiescent radio emission has been previously detected from six late-type dwarfs ranging from spectral type M7 to L3.5 (Berger et al. 2001; Berger 2002; Berger et al. 2005; Burgasser & Putman 2005; Osten et al. 2006). Four of these objects also produced short-lived, highly-polarized flares with a typical timescale of  $\sim 10$  min and a flux increase compared to the quiescent level of at least a factor of few. In addition, the L3.5 dwarf 2MASS J00361617+1821104 was shown to exhibit a periodicity of 3 hr in its quiescent radio emission, whose origin is not fully understood, but may arise from a closely-orbiting companion (Berger et al. 2005).

In the extended sample we detect radio emission from three additional dwarf stars: LHS 1070 (M5.5), LSR J1835+3259 (M8.5), and 2MASS J05233822 – 1403022 (L2.5) with fluxes of  $161 \pm 15 \mu\text{Jy}$ ,  $525 \pm 15 \mu\text{Jy}$  and  $231 \pm 14$

<sup>5</sup>The VLA is operated by the National Radio Astronomy Observatory, a facility of the National Science Foundation operated under cooperative agreement by Associated Universities, Inc.

$\mu\text{Jy}$ , respectively. LHS 1070 has been detected on two separate occasions with fluxes of  $153 \pm 23$  and  $167 \pm 20 \mu\text{Jy}$ , respectively, consistent with non-variable quiescent emission. Similarly, we do not find evidence for variability within a single observation for any of the three sources, but we note that the observations are relatively short,  $\approx 90 - 220$  min. The fractional circular polarization for the three objects is  $f_c < 30\%$  (LHS 1070),  $f_c < 9\%$  (LSR J1835+3259), and  $f_c = 19 \pm 6\%$  (2M 0523–14), similar to the level of circular polarization in the quiescent emission from previous objects.

Finally, we note that weak radio emission is detected in near positional coincidence ( $\lesssim 5''$ ) with two other sources, 2MASS J01483864 – 3024396 (M7.5) and 2MASS J04234858 – 0414035 (L7.5). However, we do not believe that these are genuine detections for two reasons. First, the offset for 2M 0423 – 04 does not coincide with the proper motion measured by Vrba et al. (2004); for 2M J0148 – 30 the proper motion is not known but the offset is  $3.3 \pm 0.4''$  with a position angle of about  $75^\circ$ . Second, in both cases the emission is strongly detected in only one of the two intermediate frequency (IF) channels of the VLA, but is consistent with zero in the other IF channel. This suggests that the radio emission is most likely spurious and may be due to a low level of interference.

#### 4. PHYSICAL PROPERTIES: MAGNETIC FIELD STRENGTH, SOURCE SIZE, AND DENSITY

Using the observed fluxes and fractional circular polarization we now estimate the magnetic field strengths for the detected sources. We first provide a rough estimate of the brightness temperature as a way to assess the origin of the radio emission (coherent vs. gyrosynchrotron):  $T_b = 2 \times 10^9 F_{\nu, \text{mJy}} \nu_{\text{GHz}}^{-2} d_{\text{pc}}^2 (R/R_J)^{-2} \text{ K}$ , where  $R_J \approx R_s \approx 7 \times 10^9 \text{ cm}$  is Jupiter's radius and roughly the source radius, and  $R \sim (1 - 2)R_J$  (Leto et al. 2000) is the size of the emitting region if the covering fraction is of order unity. For our detected sources we find  $T_b \approx 10^8 - 10^9 \text{ K}$ . Conversely, the inverse Compton limit of  $T_b \lesssim 10^{12} \text{ K}$  for gyrosynchrotron emission defines a minimum size for the emitting region of  $R \approx 0.035R_s \approx 2.5 \times 10^8 \text{ cm}$ , or about 0.03% of the surface area at the height of the corona. If the emitting region is in fact more compact than this size, then the emission is most likely due to coherent emission processes such as plasma radiation or electron cyclotron maser. Since the latter emission mechanisms are typically responsible for short-lived flares we proceed with the reasonable assumption that the observed emission is due to gyrosynchrotron radiation.

In this context we follow the typical assumption that the emitting electrons obey a power law distribution,  $N(\gamma) \propto \gamma^{-p}$  above a cutoff Lorentz factor,  $\gamma_m$ . The value of the power law index is typically  $p \sim 3$  for M dwarfs, and was found to be about 2.7 for the L3.5 dwarf 2M 0036+18 (Berger et al. 2005). We adopt the standard value of  $p = 3$  here. The peak frequency, flux, and degree of circular polarization of the detected radio emission are directly related to the density of emitting electrons ( $n_e$ ), the size of the emission region ( $R$ ), and the magnetic field strength ( $B$ ). Following the formulation of Güdel (2002) we find

that the peak frequency is given by

$$\nu_m \approx 1.66 \times 10^4 n_e^{0.23} R^{0.23} B^{0.77} \text{ Hz}, \quad (1)$$

the flux density is given by

$$F_{\nu, m} \approx 1.54 \times 10^{-4} B^{-0.76} R^2 d^{-2} \nu_m^{2.76} \mu\text{Jy}, \quad (2)$$

the fraction of circular polarization is given by

$$f_c \approx 2.85 \times 10^3 B^{0.51} \nu_m^{-0.51}, \quad (3)$$

and we assume an average angle of  $\pi/3$  between the magnetic field and the line of sight.

Using  $\nu_m = 8.5 \text{ GHz}$  as an estimate of the spectral peak, and the measured circular polarization fractions we find that  $B \approx 55 \pm 17 \text{ G}$  for 2M 0523 – 14,  $B < 135 \text{ G}$  for LHS 1070, and  $B < 13 \text{ G}$  for LSR J1835+3259. For 2M 0523 – 14 we further find a source size  $R \approx 4.6 \times 10^9 \text{ cm} \approx 0.7R_J$ , and  $n_e \approx 2.2 \times 10^9 \text{ cm}^{-3}$ . The former indicates that at the height of the emission region (presumably the corona) the field covers  $\sim 5 - 10\%$  of the surface area. For the two other sources we find  $R \lesssim 3.0 \times 10^9 \text{ cm}$  and  $n_e \gtrsim 3.3 \times 10^9 \text{ cm}^{-3}$  (LHS 1070) and  $R \lesssim 1.7 \times 10^9 \text{ cm}$  and  $n_e \gtrsim 5.8 \times 10^9 \text{ cm}^{-3}$  (LSR J1835+3259). These values, along with those inferred for the six dwarf stars detected previously, are summarized in Table 2 and Figure 2. We note that the inferred sizes are consistent with our inference based on the brightness temperature argument that the radio emission is due to gyrosynchrotron radiation,

For the non-detected sources we find a rough limit on the magnetic field strength by assuming typical values of the source size,  $0.5R_J$ , and electron density,  $n_e = 10^9 \text{ cm}^{-3}$ , as inferred from the detected sources. The resulting upper limit on the magnetic field strength is thus  $B < 9 F_{\nu, \text{mJy}}^{0.73} d_{\text{pc}}^{1.46} \text{ G}$ , which at our typical sensitivity threshold corresponds to  $B < 10^2 \text{ G}$  for  $d \lesssim 25 \text{ pc}$ ; for objects within 10 pc, the limit is  $B \lesssim 30 \text{ G}$  (Figure 2).

Thus, we find from both the detected and non-detected objects that the typical quiescent magnetic fields in late-M, L and T dwarfs are of the order of  $\lesssim 10^2 \text{ G}$ , but may approach  $\sim 1 \text{ kG}$  during flares. We note that these field strengths are relevant at the location where the radio emission is produced, possibly  $\sim 1 - 2 R_s$  above the stellar surface. Thus, depending on the exact field configuration, the surface magnetic field may be an order of magnitude larger, or nearly 1 kG even in quiescence.

The inferred field strengths can be compared to those of a few early M dwarfs (EV Lac, AD Leo, AU Mic, Gl 729) for which values of about 4 kG with a surface coverage approaching unity have been inferred from Zeeman line broadening (Saar & Linsky 1985; Johns-Krull & Valenti 1996). Somewhat weaker fields,  $\sim 1 \text{ kG}$ , have been estimated for young accreting brown dwarfs based on evidence for magnetic funneling from variations in the H $\alpha$  line (Scholz & Jayawardhana 2006). Thus, it appears that the magnetic field strengths in field late-M, L and T dwarfs may be a factor of few smaller than in early-M dwarfs, and possibly with a smaller surface coverage, but these fully convective stars and brown dwarfs are clearly capable of generating large-scale, long-lived fields.

## 5. TRENDS AND IMPLICATIONS

With the large sample of 90 M5–T8 dwarfs presented in this paper and compiled from previous work, we can begin to address trends in the radio emission, and hence magnetic properties of dwarf stars. Three interesting possibilities have been suggested previously based on a smaller sample of sources (Berger 2002). First, the ratio of radio to X-ray luminosity of late-M and L dwarfs appears to be orders of magnitude larger than that of other stars, including M dwarfs earlier than spectral type M7. Second, the level of radio activity appears to increase with later spectral type. Finally, there may be a correlation between the strength of the radio activity and rotation velocity, such that rapid rotators exhibit stronger radio activity.

We first investigate any trends in the strength of the radio activity as a function of spectral type. A proper comparison requires normalization by the bolometric luminosity of each source. These are available in the literature for about half of the survey sources, including all of the T dwarf. For the rest we use published bolometric correction factors. For the L dwarfs  $BC_K = 3.42 + 0.075(\text{SP} - 4)$  for L0–L4 and  $BC_K = 3.42 - 0.075(\text{SP} - 4)$  for L5–L9, with  $\text{SP} = 0$  for L0 (Dahn et al. 2002; Nakajima et al. 2004). For the M dwarfs we use the mean of  $BC_J = 2.43 + 0.0895\text{SP}$  and  $BC_K = 1.53 + 0.148\text{SP} - 0.0105\text{SP}^2$ , with  $\text{SP} = 0$  for M0 (Wilking et al. 1999).

With these values, we plot the ratio of radio to bolometric luminosity,  $L_{\text{rad}}/L_{\text{bol}}$ , as a function of spectral type in Figure 3. Two trends are clear from this figure. First, the fraction of detected objects drops considerably as a function of spectral type, from about 30% for the M dwarfs, to about 4% for the L dwarfs. If we consider only non-detections that are lower than the level of activity in the detected objects, these fractions are roughly 45% and 7%, respectively. Second, and perhaps more important, the level of radio activity tends to increase with later spectral types, with the active L dwarfs exhibiting a level of activity at least an order of magnitude larger than the mid-M dwarfs. Whether this trend continues to late-L and T spectral types remains unclear due to the relatively small number of observed objects and the observed decrease in the fraction of active sources. Still, the increased level of activity supports our inference that the magnetic field strengths are note significantly lower in late-M and L dwarfs.

On the other hand, with the larger sample we do not find clear evidence for a correlation between the level of activity and rotation velocity. Specifically, for the seven detected sources with a spectral type later than M7 and a measured rotation velocity, the average value of  $L_{\text{rad}}/L_{\text{bol}}$  is roughly the same for  $vsini < 20 \text{ km s}^{-1}$  and  $> 20 \text{ km s}^{-1}$ . A more careful analysis of this possible trend requires rotation velocity measurements for a significantly larger sample. As can be seen from Table 1, less than a quarter of the observed objects have measured velocities.

Finally, we find continued evidence that the correlation between radio and X-ray luminosity, which is roughly constant at a value of  $\log(L_{\text{rad}}/L_X) \sim -15.5$  for a wide range of stars (Guedel & Benz 1993; Benz & Guedel 1994), breaks down at spectral type of about M7 (Figure 4). Possible ex-

planations for the breakdown in this correlation have been discussed previously (Berger 2002; Berger et al. 2005; Osten et al. 2006), and focus on efficient trapping of the relativistic electrons, thereby reducing the efficiency of coronal and chromospheric heating, or inefficient production of X-rays due to a reduction in the number of free ions in the cool atmospheres of these dwarf stars. From a purely observational standpoint, the data indicate that the decrease in X-ray luminosity by three orders of magnitude occurs over a narrow range in spectral type at about M7 (or  $T_{\text{eff}} \approx 2500 - 2700 \text{ K}$ ), roughly the same spectral type where a transition to predominantly neutral atmospheres occurs (Mohanty et al. 2002). This is also the same location at which a significant drop in  $\text{H}\alpha$  activity occurs, from an average value of  $\log(L_{\text{H}\alpha}/L_{\text{bol}}) \approx -3.6$  earlier than M5 to  $\approx -4.3$  later than M7 (West et al. 2004). The fact that the magnetic field strengths and radio activity do not decrease significantly indicates that the drop in X-ray and  $\text{H}\alpha$  activity is related instead to the structure of the atmosphere, chromosphere and corona.

## 6. CONCLUSIONS AND FUTURE DIRECTIONS

We presented radio observations of 88 dwarf stars and brown dwarfs in the range M7–T8, along with a single M5 and a single M5.5 dwarf. This sample is nearly comparable to the number of objects with  $\text{H}\alpha$  measurements, but is significantly larger than the number of objects observed in the X-rays. The drop in the fraction of active sources at the M/L transition, which is observed in  $\text{H}\alpha$ , is also apparent in the radio observations. However, the strength of the activity in the detected objects is in fact higher for the L dwarfs, both in quiescence and during flares. As we have shown in §4, this is probably because the magnetic field strengths remain roughly unchanged despite the drop in effective temperature and luminosity with later spectral type. The implication is that the magnetic dynamo process may be similar in early-M and L dwarfs, and is not strongly dependent on luminosity or temperature.

We also stress that while  $\text{H}\alpha$  observations are relatively simple to carry out, it is not trivial to translate the observed emission to an estimate of the magnetic field strength. The advantage of radio observations is that they directly trace the strength of the field, and provide in addition information on the physical properties of the emission region, such as its size and density. We therefore suggest that a three-pronged approach is required for continued progress in our understanding of magnetic fields in dwarf stars and brown dwarfs.

First, the survey for radio emission from these objects should be expanded to all of the  $\sim 500$  currently known L and T dwarfs, as well as a large sample of objects in the spectral range M5–M9, which covers the breakdown in the radio/X-ray correlation. Such a survey can be carried out efficiently with the EVLA, which is scheduled to come online in the next few years and which will deliver a nearly order of magnitude increase in sensitivity. This is essential since the majority of the current detections are near the threshold of the VLA. We estimate that about 500–1,000 hr of observing time would be required for such an undertaking, delivering a sensitivity of  $L_{\text{rad}}/L_{\text{bol}} \sim \text{few} \times 10^{-9}$  at L0 and  $\sim 10^{-8}$  at T0.

Second, the objects that have been detected so far, and will be detected with the expanded survey, should be observed over a wide frequency range to better characterize the shape of their spectrum and the frequency dependence of their polarization. This is essential for deriving magnetic field strengths to better accuracy than is possible with the current single-frequency observations. We expect that at the current signal-to-noise level, the magnetic field strengths can be inferred to an accuracy of  $\sim 20 - 30\%$ , which is comparable to, or better than, measurements made from Zeeman broadening for early-M dwarfs. In addition, long timescale, high signal-to-noise observations can be used to check for possible periodicity in the radio emission, as has been uncovered for the L3.5 dwarf 2M 0036+18 (Berger et al. 2005). If the periodicity is in fact related to a close-in companion, which excites the dynamo by tidal or magnetic interactions, this may be a ubiquitous feature of the active objects.

Finally, these same objects should be observed simultaneously in the radio, X-rays, and H $\alpha$  in order to directly measure the correlation, or lack thereof, between these activity indicators. This is necessary in order to trace the origin of the shift in the radio/X-ray correlation, and in

order to trace the evolution of flares as the release of magnetic stresses, evident in the radio, heats up the corona (X-rays) and chromosphere (H $\alpha$ ). While the current observations allow us to address in a statistical manner the overall trends observed with each technique, only simultaneous observations can provide insight into the production and evolution of flares. As the most catastrophic events in the atmospheres of dwarf stars, such events will undoubtedly shed light on the structure of the fields, their strengths, and the details of the energy dissipation process, all of which will provide observational constraints on the dynamo mechanism in dwarf stars.

Research has benefitted from the M, L, and T dwarf compendium housed at DwarfArchives.org and maintained by Chris Gelino, Davy Kirkpatrick, and Adam Burgasser. This work has made use of the SIMBAD database, operated at CDS, Strasbourg, France. E.B. is supported by NASA through Hubble Fellowship grant HST-01171.01 awarded by the Space Telescope Science Institute, which is operated by AURA, Inc., for NASA under contract NAS 5-26555.

#### References

Audard, M., Brown, A., Briggs, K. R., Güdel, M., Telleschi, A., & Gizis, J. E. 2005, ApJ, 625, L63

Bailer-Jones, C. A. L. 2004, A&A, 419, 703

Basri, G., & Marcy, G. W. 1995, AJ, 109, 762

Benz, A. O., & Guedel, M., 285, 621

Berger, E. 2002, ApJ, 572, 503

Berger, E., et al. 2001, Nature, 410, 338

Berger, E., et al. 2005, ApJ, 627, 960

Bouy, H., Brandner, W., Martín, E. L., Delfosse, X., Allard, F., & Basri, G. 2003, AJ, 126, 1526

Bouy, H., et al. 2004, A&A, 423, 341

Burgasser, A. J., et al. 1999, ApJ, 522, L65

Burgasser, A. J., Kirkpatrick, J. D., Liebert, J., & Burrows, A. 2003a, ApJ, 594, 510

Burgasser, A. J., Kirkpatrick, J. D., McElwain, M. W., Cutri, R. M., Burgasser, A. J., & Skrutskie, M. F. 2003b, AJ, 125, 850

Burgasser, A. J., Kirkpatrick, J. D., Reid, I. N., Brown, M. E., Miskey, C. L., & Gizis, J. E. 2003c, ApJ, 586, 512

Burgasser, A. J., & Putman, M. E. 2005, ApJ, 626, 486

Burgasser, A. J., Reid, I. N., Leggett, S. K., Kirkpatrick, J. D., Liebert, J., & Burrows, A. 2005, ApJ, 634, L177

Burgasser, A. J., et al. 2000, AJ, 120, 1100

Costa, E., Méndez, R. A., Jao, W.-C., Henry, T. J., Subasavage, J. P., Brown, M. A., Ianna, P. A., & Bartlett, J. 2005, AJ, 130, 337

Cruz, K. L., & Reid, I. N. 2002, AJ, 123, 2828

Cruz, K. L., Reid, I. N., Liebert, J., Kirkpatrick, J. D., & Lowrance, P. J. 2003, AJ, 126, 2421

Dahn, C. C., et al. 2002, AJ, 124, 1170

Deacon, N. R., & Hambly, N. C. 2001, *A&A*, 380, 148

Delfosse, X., Tinney, C. G., Forveille, T., Epchtein, N., Borsenberger, J., Fouqué, P., Kimeswenger, S., & Tiphène, D. 1999, *A&AS*, 135, 41

Dobler, W., Stix, M., & Brandenburg, A. 2006, *ApJ*, 638, 336

Durney, B. R., De Young, D. S., & Roxburgh, I. W., 145, 207

Fleming, T. A., Giampapa, M. S., Schmitt, J. H. M. M., & Bookbinder, J. A. 1993, *ApJ*, 410, 387

Fuhrmeister, B., & Schmitt, J. H. M. M. 2004, *A&A*, 420, 1079

Geballe, T. R., et al. 2002, *ApJ*, 564, 466

Gizis, J. E. 2002, *ApJ*, 575, 484

Gizis, J. E., Monet, D. G., Reid, I. N., Kirkpatrick, J. D., Liebert, J., & Williams, R. J. 2000, *AJ*, 120, 1085

Gizis, J. E., & Reid, I. N. 2006, *AJ*, 131, 638

Golimowski, D. A., et al. 2004, *AJ*, 127, 3516

Graham, J. R., Matthews, K., Greenstein, J. L., Neugebauer, G., Tinney, C. G., & Persson, S. E. 1992, *AJ*, 104, 2016

Güdel, M. 2002, *ARA&A*, 40, 217

Guedel, M., & Benz, A. O. 1993, *ApJ*, 405, L63

Guedel, M., Benz, A. O., Schmitt, J. H. M. M., & Skinner, S. L. 1996, *ApJ*, 471, 1002

Hawley, S. L., et al. 2002, *AJ*, 123, 3409

Hawley, S. L., et al. 1995, *ApJ*, 453, 464

Johns-Krull, C. M., & Valenti, J. A. 1996, *ApJ*, 459, L95

Kendall, T. R., Delfosse, X., Martín, E. L., & Forveille, T. 2004, *A&A*, 416, L17

Kendall, T. R., Mauron, N., Azzopardi, M., & Gigoyan, K. 2003, *A&A*, 403, 929

Kirkpatrick, J. D. 2005, *ARA&A*, 43, 195

Kirkpatrick, J. D., Dahn, C. C., Monet, D. G., Reid, I. N., Gizis, J. E., Liebert, J., & Burgasser, A. J. 2001, *AJ*, 121, 3235

Kirkpatrick, J. D., Henry, T. J., & Liebert, J. 1993, *ApJ*, 406, 701

Kirkpatrick, J. D., et al. 2000, *AJ*, 120, 447

Knapp, G. R., et al. 2004, *AJ*, 127, 3553

Krishnamurthi, A., Leto, G., & Linsky, J. L. 1999, *AJ*, 118, 1369

Leggett, S. K., et al. 2002, *ApJ*, 564, 452

Leto, G., Pagano, I., Linsky, J. L., Rodonò, M., & Umana, G. 2000, *A&A*, 359, 1035

Liebert, J., Kirkpatrick, J. D., Cruz, K. L., Reid, I. N., Burgasser, A., Tinney, C. G., & Gizis, J. E. 2003, *AJ*, 125, 343

Lodieu, N., Scholz, R.-D., & McCaughrean, M. J. 2002, *A&A*, 389, L20

Lodieu, N., Scholz, R.-D., McCaughrean, M. J., Ibata, R., Irwin, M., & Zinnecker, H. 2005, *A&A*, 440, 1061

Martín, E. L., & Ardila, D. R. 2001, *AJ*, 121, 2758

Martín, E. L., Delfosse, X., Basri, G., Goldman, B., Forveille, T., & Zapatero Osorio, M. R. 1999, *AJ*, 118, 2466

Martín, E. L., Dougados, C., Magnier, E., Ménard, F., Magazzù, A., Cuillandre, J.-C., & Delfosse, X. 2001, *ApJ*, 561, L195

McCaughrean, M. J., Close, L. M., Scholz, R.-D., Lenzen, R., Biller, B., Brandner, W., Hartung, M., & Lodieu, N. 2004, *A&A*, 413, 1029

Mohanty, S., & Basri, G. 2003, *ApJ*, 583, 451

Mohanty, S., Basri, G., Shu, F., Allard, F., & Chabrier, G. 2002, *ApJ*, 571, 469

Mullan, D. J., & MacDonald, J. 2001, *ApJ*, 559, 353

Nakajima, T., Oppenheimer, B. R., Kulkarni, S. R., Golimowski, D. A., Matthews, K., & Durrance, S. T. 1995, *Nature*, 378, 463

Nakajima, T., Tsuji, T., & Yanagisawa, K. 2004, *ApJ*, 607, 499

Neuhäuser, R., et al. 1999, *A&A*, 343, 883

Neupert, W. M. 1968, *ApJ*, 153, L59

Oppenheimer, B. R., Kulkarni, S. R., Matthews, K., & Nakajima, T. 1995, *Science*, 270, 1478

Osten, R. A., Hawley, S. L., Bastian, T. S., & Reid, I. N. 2006, *ApJ*, 637, 518

Pizzolato, N., Maggio, A., Micela, G., Sciortino, S., & Ventura, P. 2003, *A&A*, 397, 147

Raedler, K.-H., Wiedemann, E., Meinel, R., Brandenburg, A., & Tuominen, I. 1990, *A&A*, 239, 413

Reid, I. N., et al. 2003a, *AJ*, 126, 3007

Reid, I. N., et al. 2003b, *AJ*, 125, 354

Reid, I. N., Kirkpatrick, J. D., Gizis, J. E., Dahn, C. C., Monet, D. G., Williams, R. J., Liebert, J., & Burgasser, A. J. 2000, *AJ*, 119, 369

Reid, I. N., Kirkpatrick, J. D., Gizis, J. E., & Liebert, J. 1999, *ApJ*, 527, L105

Reid, I. N., Kirkpatrick, J. D., Liebert, J., Gizis, J. E., Dahn, C. C., & Monet, D. G. 2002, *AJ*, 124, 519

Reid, N. 2003, *MNRAS*, 342, 837

Reiners, A., & Basri, G. 2006, ArXiv Astrophysics e-prints

Rosner, R., Golub, L., & Vaiana, G. S. 1985, *ARA&A*, 23, 413

Ruiz, M. T., Leggett, S. K., & Allard, F. 1997, *ApJ*, 491, L107

Rutledge, R. E., Basri, G., Martín, E. L., & Bildsten, L. 2000, *ApJ*, 538, L141

Saar, S. H., & Linsky, J. L. 1985, *ApJ*, 299, L47

Salim, S., & Gould, A. 2003, *ApJ*, 582, 1011

Salim, S., Lépine, S., Rich, R. M., & Shara, M. M. 2003, *ApJ*, 586, L149

Scholz, A., & Jayawardhana, R. 2006, *ApJ*, 638, 1056

Scholz, R.-D., McCaughrean, M. J., Lodieu, N., & Kuhlbrot, B. 2003, *A&A*, 398, L29

Schweitzer, A., Gizis, J. E., Hauschildt, P. H., Allard, F., & Reid, I. N. 2001, *ApJ*, 555, 368

Smith, V. V., et al. 2003, *ApJ*, 599, L107

Tinney, C. G. 1998, *MNRAS*, 296, L42

Tinney, C. G., Burgasser, A. J., & Kirkpatrick, J. D. 2003, *AJ*, 126, 975

Tinney, C. G., Delfosse, X., & Forveille, T. 1997, *ApJ*, 490, L95

Tsvetanov, Z. I., et al. 2000, *ApJ*, 531, L61

Vrba, F. J., et al. 2004, *AJ*, 127, 2948

West, A. A., et al. 2004, *AJ*, 128, 426

Wilking, B. A., Greene, T. P., & Meyer, M. R. 1999, *AJ*, 117, 469

Zapatero Osorio, M. R., Béjar, V. J. S., Martín, E. L., Rebolo, R., Barrado y Navascués, D., Bailer-Jones, C. A. L., & Mundt, R. 2000, *Science*, 290, 103

TABLE 1  
RADIO OBSERVATIONS OF M,L,T DWARFS

RA	Dec	SpT	<i>J</i> (mag)	<i>K</i> (mag)	$\pi$ (mas)	$F_{\nu, R}$ (μJy)	$vsini$ (km s $^{-1}$ )	$L_{bol}$ ( $L_{\odot}$ )	$L_{H\alpha}/L_{bol}$	$R$ ( $R_{\odot}$ )	$T$ (K)	Notes
16 <sup>h</sup> 26 <sup>m</sup> 19.2 <sup>s</sup>	-24 <sup>o</sup> 24'16"	M5	16.35	11.73	6.25	< 150	...	-1.32	...	...	...	[1]
00 <sup>h</sup> 24 <sup>m</sup> 44.2 <sup>s</sup>	-27 <sup>o</sup> 08'24"	M5.5	9.26	8.23	135.3	161 ± 15	...	...	...	...	...	LHS 1070ABC
04 <sup>h</sup> 35 <sup>m</sup> 16.1 <sup>s</sup>	-16 <sup>o</sup> 06'57"	M7	10.40	9.34	116.3	< 48	...	...	-4.71 <sup>a</sup>	...	...	LP 775-31
04 <sup>h</sup> 40 <sup>m</sup> 23.2 <sup>s</sup>	-05 <sup>o</sup> 30'08"	M7	10.68	9.56	102.0	< 39	...	...	-4.28 <sup>a</sup>	...	...	LP 655-48
07 <sup>h</sup> 52 <sup>m</sup> 23.9 <sup>s</sup>	+16 <sup>o</sup> 12'16"	M7	10.83	9.82	95.2	< 39	...	...	...	...	...	LP 423-31
14 <sup>h</sup> 56 <sup>m</sup> 38.3 <sup>s</sup>	-28 <sup>o</sup> 09'47"	M7	9.96	8.92	152.4	270 ± 40	8	-3.29	-5.22	...	2600	[2], LHS 3003
16 <sup>h</sup> 55 <sup>m</sup> 35.3 <sup>s</sup>	-08 <sup>o</sup> 23'40"	M7	9.78	8.83	154.5	< 24	9	-3.21	-4.06	0.113	2707	[3], VB8
01 <sup>h</sup> 48 <sup>m</sup> 38.6 <sup>s</sup>	-30 <sup>o</sup> 24'40"	M7.5	12.28	11.24	54.3	< 45	...	...	...	...	...	...
03 <sup>h</sup> 31 <sup>m</sup> 30.2 <sup>s</sup>	-30 <sup>o</sup> 42'38"	M7.5	11.37	10.28	82.6	< 72	...	...	-4.21 <sup>a</sup>	...	...	LP 888-18
04 <sup>h</sup> 17 <sup>m</sup> 37.5 <sup>s</sup>	-08 <sup>o</sup> 00'01"	M7.5	12.17	11.05	57.5	< 36	...	...	...	...	...	...
04 <sup>h</sup> 29 <sup>m</sup> 18.4 <sup>s</sup>	-31 <sup>o</sup> 23'57"	M7.5	10.89	9.80	103.1	< 48	...	...	...	...	...	...
15 <sup>h</sup> 21 <sup>m</sup> 01.0 <sup>s</sup>	+50 <sup>o</sup> 53'23"	M7.5	12.00	10.92	62.1	< 39	...	...	...	...	...	...
10 <sup>h</sup> 16 <sup>m</sup> 34.7 <sup>s</sup>	+27 <sup>o</sup> 51'50"	M7.5	11.95	10.95	63.3	< 45	7	...	-4.70	...	...	[1], LHS 2243
19 <sup>h</sup> 16 <sup>m</sup> 57.6 <sup>s</sup>	+05 <sup>o</sup> 09'02"	M8	9.95	8.81	174.2	< 81	6.5	-3.35	-4.32	...	2700	[3], VB10
15 <sup>h</sup> 34 <sup>m</sup> 57.0 <sup>s</sup>	-14 <sup>o</sup> 18'48"	M8	11.39	10.31	90.9	< 111	...	-3.39	-4.80 <sup>a</sup>	...	2500	[2]
10 <sup>h</sup> 48 <sup>m</sup> 14.2 <sup>s</sup>	-39 <sup>o</sup> 56'09"	M8	9.55	8.45	247.5	140 ± 40	25	-3.39	-4.92 <sup>a</sup>	...	2500	[2]
$(29.6 \pm 1) \times 10^4$												
11 <sup>h</sup> 39 <sup>m</sup> 51.1 <sup>s</sup>	-31 <sup>o</sup> 59'21"	M8	12.67	11.49	50	< 99	...	-3.39	-4.22 <sup>a</sup>	...	2500	[2]
18 <sup>h</sup> 43 <sup>m</sup> 22.1 <sup>s</sup>	+40 <sup>o</sup> 40'21"	M8	11.30	10.27	70.9	< 48	...	-3.10	...	...	...	LHS 3406
00 <sup>h</sup> 19 <sup>m</sup> 26.3 <sup>s</sup>	+46 <sup>o</sup> 14'08"	M8	12.61	11.47	51.3	< 33	...	...	...	...	...	...
03 <sup>h</sup> 50 <sup>m</sup> 57.4 <sup>s</sup>	+18 <sup>o</sup> 18'07"	M8	12.95	11.76	43.7	< 105	4	...	-4.06	...	2550	LP 413-53
04 <sup>h</sup> 36 <sup>m</sup> 10.4 <sup>s</sup>	+22 <sup>o</sup> 59'56"	M8	13.76	12.19	7.14	< 45	8	...	-4.36 <sup>a</sup>	...	...	CFHT-BD-tau-2
05 <sup>h</sup> 17 <sup>m</sup> 37.7 <sup>s</sup>	-33 <sup>o</sup> 49'03"	M8	12.00	10.82	68.0	< 54	...	...	...	...	...	DENIS 0517 - 33
20 <sup>h</sup> 37 <sup>m</sup> 07.1 <sup>s</sup>	-11 <sup>o</sup> 37'57"	M8	12.28	11.26	59.5	< 33	...	...	...	...	...	...
15 <sup>h</sup> 01 <sup>m</sup> 08.3 <sup>s</sup>	+22 <sup>o</sup> 50'02"	M8.5	11.80	10.74	94.4	190 ± 15	60	-3.59	-5.03	0.097	2319	[1], TVLM 513-46 flare
$980 \pm 40$												
03 <sup>h</sup> 35 <sup>m</sup> 02.1 <sup>s</sup>	+23 <sup>o</sup> 42'36"	M8.5	12.26	11.26	52.1	< 69	30	...	-4.63	...	2475	...
18 <sup>h</sup> 35 <sup>m</sup> 37.9 <sup>s</sup>	+32 <sup>o</sup> 59'55"	M8.5	10.27	9.15	176.4	525 ± 15	...	...	...	...	...	LSR 1835+3259
14 <sup>h</sup> 54 <sup>m</sup> 28.0 <sup>s</sup>	+16 <sup>o</sup> 06'05"	M8.5	11.14	10.02	101.9	< 30	...	-3.39	...	...	2440	[3], GJ 569Ba
14 <sup>h</sup> 54 <sup>m</sup> 28.0 <sup>s</sup>	+16 <sup>o</sup> 06'05"	M9	11.65	10.43	101.9	< 30	...	-3.56	...	...	2305	[3], GJ 569Bb
08 <sup>h</sup> 53 <sup>m</sup> 36.2 <sup>s</sup>	-03 <sup>o</sup> 29'32"	M9	11.18	9.97	117.6	< 81	12	-3.49	-4.30	0.101	2441	[1,3], LHS 2065
01 <sup>h</sup> 09 <sup>m</sup> 51.2 <sup>s</sup>	-03 <sup>o</sup> 43'26"	M9	11.70	10.42	90.9	< 33	...	...	-4.52 <sup>a</sup>	...	...	LP 647-13
04 <sup>h</sup> 34 <sup>m</sup> 15.2 <sup>s</sup>	+22 <sup>o</sup> 50'31"	M9	13.74	11.87	7.14	< 69	7	...	-4.55 <sup>a</sup>	...	...	CFHT-BD-tau-1
04 <sup>h</sup> 36 <sup>m</sup> 38.9 <sup>s</sup>	+22 <sup>o</sup> 58'12"	M9	13.70	12.34	7.14	< 57	12	...	-3.79 <sup>a</sup>	...	...	CFHT-BD-tau-3
05 <sup>h</sup> 37 <sup>m</sup> 25.9 <sup>s</sup>	-02 <sup>o</sup> 34'32"	M9	18.22	17.00	2.84	< 66	...	-3.08	-3.00	...	2460	SOri 55
17 <sup>h</sup> 07 <sup>m</sup> 23.4 <sup>s</sup>	-05 <sup>o</sup> 58'24"	M9	12.06	10.71	...	< 48	...	...	-5.82 <sup>a</sup>	...	...	...
00 <sup>h</sup> 19 <sup>m</sup> 45.8 <sup>s</sup>	+52 <sup>o</sup> 13'18"	M9	12.82	11.62	53.5	< 42	...	...	...	...	...	...
03 <sup>h</sup> 39 <sup>m</sup> 35.2 <sup>s</sup>	-35 <sup>o</sup> 25'44"	M9	10.75	9.52	201.4	74 ± 13	28	-3.79	-5.26	0.093	2138	[4], LP 944-20 flare
$2600 \pm 200$												
04 <sup>h</sup> 43 <sup>m</sup> 37.6 <sup>s</sup>	+00 <sup>o</sup> 02'05"	M9.5	12.52	11.17	65.4	< 60	...	...	...	...	...	...
00 <sup>h</sup> 24 <sup>m</sup> 24.6 <sup>s</sup>	-01 <sup>o</sup> 58'20"	M9.5	11.86	10.58	86.6	83 ± 18	34	-3.45	< -6.01	0.103	2495	[1], BRI 0021-0214
00 <sup>h</sup> 27 <sup>m</sup> 42.0 <sup>s</sup>	+05 <sup>o</sup> 03'41"	M9.5	16.08	14.87	13.8	< 75	13	-3.62	-3.39	0.097	2302	[1], PC 0025+0447
03 <sup>h</sup> 45 <sup>m</sup> 43.1 <sup>s</sup>	+25 <sup>o</sup> 40'23"	L0	13.92	12.67	37.1	< 87	25	-3.56	...	0.098	2364	[1]
07 <sup>h</sup> 46 <sup>m</sup> 42.5 <sup>s</sup>	+20 <sup>o</sup> 00'32"	L0.5	11.78	10.47	81.9	< 48	24	-3.62	-5.24	0.097	2302	...
06 <sup>h</sup> 02 <sup>m</sup> 30.4 <sup>s</sup>	+39 <sup>o</sup> 10'59"	L1	12.30	10.86	94.3	< 30	...	...	...	...	...	LSR 0602+3910
13 <sup>h</sup> 00 <sup>m</sup> 42.5 <sup>s</sup>	+19 <sup>o</sup> 12'35"	L1	12.72	11.62	71.9	< 87	...	...	...	...	...	...
18 <sup>h</sup> 07 <sup>m</sup> 15.9 <sup>s</sup>	+50 <sup>o</sup> 15'31"	L1.5	12.93	11.60	68.5	< 39	...	...	...	...	...	...
02 <sup>h</sup> 13 <sup>m</sup> 28.8 <sup>s</sup>	+44 <sup>o</sup> 44'45"	L1.5	13.49	12.21	53.5	< 30	...	...	...	...	...	...
20 <sup>h</sup> 57 <sup>m</sup> 54.0 <sup>s</sup>	-02 <sup>o</sup> 52'30"	L1.5	13.12	11.72	61.7	< 36	...	...	...	...	...	DENIS 2057 - 02
04 <sup>h</sup> 45 <sup>m</sup> 53.8 <sup>s</sup>	-30 <sup>o</sup> 48'20"	L2	13.41	11.98	60.2	< 66	...	...	...	...	...	...
01 <sup>h</sup> 09 <sup>m</sup> 01.5 <sup>s</sup>	-51 <sup>o</sup> 00'49"	L2	12.23	11.09	100	< 111	...	-3.89	...	...	2100	[2]
13 <sup>h</sup> 05 <sup>m</sup> 40.1 <sup>s</sup>	-25 <sup>o</sup> 41'10"	L2	13.41	11.75	53.6	< 27	60	-3.57	-5.23	0.098	2354	[3], Kelu 1
05 <sup>h</sup> 23 <sup>m</sup> 38.2 <sup>s</sup>	-14 <sup>o</sup> 03'02"	L2.5	13.08	11.64	74.6	< 39	...	...	...	...	...	...
05 <sup>h</sup> 23 <sup>m</sup> 38.2 <sup>s</sup>	-14 <sup>o</sup> 03'02"	L2.5	13.08	11.64	74.6	231 ± 14	...	...	...	...	...	...
17 <sup>h</sup> 21 <sup>m</sup> 03.9 <sup>s</sup>	+33 <sup>o</sup> 44'16"	L3	13.62	12.49	65.8	< 48	...	...	...	...	...	...
02 <sup>h</sup> 51 <sup>m</sup> 14.9 <sup>s</sup>	-03 <sup>o</sup> 52'45"	L3	13.06	11.66	82.6	< 36	...	...	...	...	...	...
21 <sup>h</sup> 04 <sup>m</sup> 14.9 <sup>s</sup>	-10 <sup>o</sup> 37'36"	L3	13.84	12.37	58.1	< 24	...	...	...	...	...	...
00 <sup>h</sup> 45 <sup>m</sup> 21.4 <sup>s</sup>	+16 <sup>o</sup> 34'44"	L3.5	13.06	11.37	96.2	< 39	...	...	...	...	...	...
00 <sup>h</sup> 36 <sup>m</sup> 16.1 <sup>s</sup>	+18 <sup>o</sup> 21'10"	L3.5	12.47	11.06	114.2	134 ± 16	15	-3.93	0	0.091	1993	[1,5] flare
$720 \pm 40$												
17 <sup>h</sup> 05 <sup>m</sup> 48.3 <sup>s</sup>	-05 <sup>o</sup> 16'46"	L4	13.31	12.03	93.4	< 45	...	...	...	...	...	DENIS 1705 - 05
14 <sup>h</sup> 24 <sup>m</sup> 39.0 <sup>s</sup>	+09 <sup>o</sup> 17'10"	L4	15.69	14.17	31.7	< 96	17.5	-4.04	-5.07	0.090	1885	[1], GD 165B

TABLE 1—Continued

RA	Dec	SpT	<i>J</i> (mag)	<i>K</i> (mag)	$\pi$ (mas)	$F_{\nu, R}$ ( $\mu$ Jy)	$v \sin i$ (km s $^{-1}$ )	$L_{\text{bol}}$ ( $L_{\odot}$ )	$L_{\text{H}\alpha}/L_{\text{bol}}$	$R$ ( $R_{\odot}$ )	$T$ (K)	Notes
06 <sup>h</sup> 52 <sup>m</sup> 30.7 <sup>s</sup>	+47 <sup>°</sup> 10'34"	L4.5	13.54	11.69	90.1	< 33	...	...	...	...	...	...
22 <sup>h</sup> 24 <sup>m</sup> 43.8 <sup>s</sup>	-01 <sup>°</sup> 58'52"	L4.5	14.07	12.02	88.1	< 33	...	-4.13	...	0.089	1792	
01 <sup>h</sup> 41 <sup>m</sup> 03.2 <sup>s</sup>	+18 <sup>°</sup> 04'50"	L4.5	13.88	12.49	79.4	< 30	...	...	...	...	...	
08 <sup>h</sup> 35 <sup>m</sup> 42.5 <sup>s</sup>	-08 <sup>°</sup> 19'23"	L5	13.17	11.14	109.9	< 30	...	-4.09	...	...	1700	
01 <sup>h</sup> 44 <sup>m</sup> 35.3 <sup>s</sup>	-07 <sup>°</sup> 16'14"	L5	14.19	12.27	74.6	< 33	...	...	...	...	...	
02 <sup>h</sup> 05 <sup>m</sup> 03.4 <sup>s</sup>	+12 <sup>°</sup> 51'42"	L5	15.68	13.67	37.0	< 48	...	...	...	...	...	
00 <sup>h</sup> 04 <sup>m</sup> 34.8 <sup>s</sup>	-40 <sup>°</sup> 44'05"	L5	13.11	11.40	104.7	< 45	32.5	-4.00	-5.23	0.090	1923	LHS 102B
15 <sup>h</sup> 07 <sup>m</sup> 47.6 <sup>s</sup>	-16 <sup>°</sup> 27'38"	L5	12.82	11.31	136.4	< 57	...	-4.23	...	0.088	1703	
12 <sup>h</sup> 28 <sup>m</sup> 15.2 <sup>s</sup>	-15 <sup>°</sup> 47'34"	L5	14.38	12.77	49.4	< 87	22	-4.19	-5.75	0.089	1734	[1], DENIS 1228 – 15
15 <sup>h</sup> 15 <sup>m</sup> 00.8 <sup>s</sup>	+48 <sup>°</sup> 47'41"	L6	14.06	12.56	108.7	< 27	...	...	...	...	...	
04 <sup>h</sup> 39 <sup>m</sup> 01.0 <sup>s</sup>	-23 <sup>°</sup> 53'08"	L6.5	14.41	12.82	92.6	< 42	...	...	...	...	...	
02 <sup>h</sup> 05 <sup>m</sup> 29.4 <sup>s</sup>	-11 <sup>°</sup> 59'29"	L7	14.59	13.00	50.6	< 30	22	-4.34	< -6.16	0.088	1601	DENIS 0205 – 11
00 <sup>h</sup> 30 <sup>m</sup> 30.0 <sup>s</sup>	-14 <sup>°</sup> 50'33"	L7	16.28	14.48	37.4	< 57	...	...	...	...	...	
17 <sup>h</sup> 28 <sup>m</sup> 11.4 <sup>s</sup>	+39 <sup>°</sup> 48'59"	L7	15.99	13.91	41.5	< 54	...	...	...	...	...	
08 <sup>h</sup> 25 <sup>m</sup> 19.6 <sup>s</sup>	+21 <sup>°</sup> 15'52"	L7.5	15.10	13.03	93.8	< 45	...	-4.61	...	0.088	1372	
04 <sup>h</sup> 23 <sup>m</sup> 48.5 <sup>s</sup>	-04 <sup>°</sup> 14'03"	L7.5	14.46	12.93	65.9	< 42	...	...	...	...	...	
22 <sup>h</sup> 52 <sup>m</sup> 10.7 <sup>s</sup>	-17 <sup>°</sup> 30'13"	L7.5	14.31	12.90	120.5	< 30	...	...	...	...	...	DENIS 2252 – 17
09 <sup>h</sup> 29 <sup>m</sup> 33.6 <sup>s</sup>	+34 <sup>°</sup> 29'52"	L8	16.60	14.64	45.5	< 42	...	...	...	...	...	
15 <sup>h</sup> 23 <sup>m</sup> 22.6 <sup>s</sup>	+30 <sup>°</sup> 14'56"	L8	16.06	14.35	53.7	< 45	...	-4.60	...	0.088	1376	Gl 584C
16 <sup>h</sup> 32 <sup>m</sup> 29.1 <sup>s</sup>	+19 <sup>°</sup> 04'41"	L8	15.87	14.00	65.6	< 54	30	-4.65	-6.23	0.088	1335	
01 <sup>h</sup> 51 <sup>m</sup> 41.5 <sup>s</sup>	+12 <sup>°</sup> 44'30"	T0.5	16.57	15.18	46.7	< 51	...	-4.68	...	...	1300	
22 <sup>h</sup> 04 <sup>m</sup> 10.5 <sup>s</sup>	-56 <sup>°</sup> 46'57"	T1	12.29	11.35	275.8	< 79	28	-4.71	...	0.091	1276	[6], eInd Ba
02 <sup>h</sup> 07 <sup>m</sup> 42.8 <sup>s</sup>	+00 <sup>°</sup> 00'56"	T4.5	16.80	15.41	34.8	< 39	...	-4.82	...	...	1200	
05 <sup>h</sup> 59 <sup>m</sup> 19.1 <sup>s</sup>	-14 <sup>°</sup> 04'48"	T4.5	13.80	13.58	97.7	< 27	...	-4.53	...	...	1425	
15 <sup>h</sup> 34 <sup>m</sup> 49.8 <sup>s</sup>	-29 <sup>°</sup> 52'27"	T5.5	14.90	14.84	73.6	< 63	...	-5.00	...	...	1070	
16 <sup>h</sup> 24 <sup>m</sup> 14.4 <sup>s</sup>	+00 <sup>°</sup> 29'16"	T6	15.49	15.52	90.9	< 36	...	-5.16	...	...	975	
22 <sup>h</sup> 04 <sup>m</sup> 10.5 <sup>s</sup>	-56 <sup>°</sup> 46'57"	T1	13.23	13.53	275.8	< 79	...	-5.35	...	0.096	854	[6], eInd Bb
13 <sup>h</sup> 46 <sup>m</sup> 46.4 <sup>s</sup>	-00 <sup>°</sup> 31'50"	T6.5	16.00	15.77	68.3	< 105	...	-5.00	...	...	1075	[1]
10 <sup>h</sup> 47 <sup>m</sup> 53.9 <sup>s</sup>	+21 <sup>°</sup> 24'23"	T6.5	15.82	16.41	94.7	< 45	...	-5.35	...	...	900	
06 <sup>h</sup> 10 <sup>m</sup> 35.1 <sup>s</sup>	-21 <sup>°</sup> 51'17"	T7	14.20	14.30	173.2	< 69	...	-5.21	...	...	950	[3], Gl 229B
12 <sup>h</sup> 17 <sup>m</sup> 11.1 <sup>s</sup>	-03 <sup>°</sup> 11'13"	T7.5	15.86	15.89	90.8	< 111	...	-5.32	...	...	900	
04 <sup>h</sup> 15 <sup>m</sup> 19.5 <sup>s</sup>	-09 <sup>°</sup> 35'06"	T8	15.70	15.43	174.3	< 45	...	-5.73	...	...	700	

NOTE.—Properties of the M,L,T dwarfs presented in this paper. The columns are (left to right): (i) right ascension, (ii) declination, (iii) spectral type, (iv) *J*-band magnitude, (v) *K*-band magnitude, (vi) parallax, (vii) radio flux, (viii) rotation velocity, (ix) bolometric luminosity, (x)  $\text{H}\alpha$  activity, (xi) radius, (xii) surface temperature, and (xiii) notes: [1] Berger (2002), [2] Burgasser & Putman (2005), [3] Krishnamurthi et al. (1999), [4] Berger et al. (2001), [5] Berger et al. (2005), [6] Audard et al. (2005). <sup>a</sup>:  $L_{\text{H}\alpha}/L_{\text{bol}}$  calculated from the  $\text{H}\alpha$  line equivalent width using the conversion of West et al. (2004). References for source properties: Wilking et al. (1999), Cruz & Reid (2002), Cruz et al. (2003), Lodieu et al. (2005), Reid et al. (2003a), Dahn et al. (2002), Mohanty & Basri (2003), Reid (2003), Gizis (2002), Fuhrmeister & Schmitt (2004), Deacon & Hambley (2001), Gizis et al. (2000), Martín et al. (2001), Leggett et al. (2002), Golimowski et al. (2004), Geballe et al. (2002), Reid et al. (2002), Reid et al. (2003b), Costa et al. (2005), Salim & Gould (2003), Liebert et al. (2003), Zapatero Osorio et al. (2000), Martín & Ardila (2001), Neuhauser et al. (1999), Graham et al. (1992), Knapp et al. (2004), Hawley et al. (2002), Martín et al. (1999), Gizis & Reid (2006), Bouy et al. (2004), Salim et al. (2003), Kirkpatrick (2005), Lodieu et al. (2002), Bailer-Jones (2004), Ruiz et al. (1997), Tinney (1998), Kendall et al. (2004), Schweitzer et al. (2001), Reid et al. (2000), Kirkpatrick et al. (2000), Kirkpatrick et al. (1993), Kendall et al. (2003), Burgasser et al. (2005), Delfosse et al. (1999), Tinney et al. (1997), Kirkpatrick et al. (2001), Scholz et al. (2003), McCaughrean et al. (2004), Tinney et al. (2003), Smith et al. (2003), Burgasser et al. (2000), Burgasser et al. (2003b), Burgasser et al. (2003a), Burgasser et al. (2003c), Tsvetanov et al. (2000), Bouy et al. (2003), Burgasser et al. (1999), Nakajima et al. (1995), Oppenheimer et al. (1995).

TABLE 2  
PHYSICAL PROPERTIES OF M AND L DWARFS

Object	Sp. Type	Quiescent			Flaring		
		$B$ (G)	$R$ (cm)	$n_e$ (cm $^{-3}$ )	$B$ (G)	$R$ (cm)	$n_e$ (cm $^{-3}$ )
LHS 1070	M5.5	< 135	< $3.0 \times 10^9$	> $3.3 \times 10^9$	...	...	...
DENIS 1048	M8	...	...	...	$2 \times 10^3$	< $3 \times 10^8$	$3 \times 10^{11}$
TVLM 513	M8.5	< 35	< $3.0 \times 10^9$	> $1.5 \times 10^{10}$	630	$1.9 \times 10^{10}$	$1.5 \times 10^5$
LSR 1835+32	M8.5	< 13	< $1.7 \times 10^9$	> $5.8 \times 10^9$	...	...	...
LP 944-20	M9.5	< 95	< $1.2 \times 10^9$	> $1.3 \times 10^9$	135	$7.1 \times 10^9$	$6.9 \times 10^7$
BRI 0021	M9.5	95	$3.0 \times 10^9$	$5.3 \times 10^8$	...	...	...
2M 0523 – 14	L2.5	55	$4.6 \times 10^9$	$2.2 \times 10^9$	...	...	...
2M 0036+18	L3.5	175	$1.0 \times 10^{10}$	$1.6 \times 10^6$	560	$1.3 \times 10^{10}$	$3.2 \times 10^5$

NOTE.—Derived magnetic field strengths, as well as electron densities and emission region sizes for the M and L dwarfs presented in this paper and in the literature.

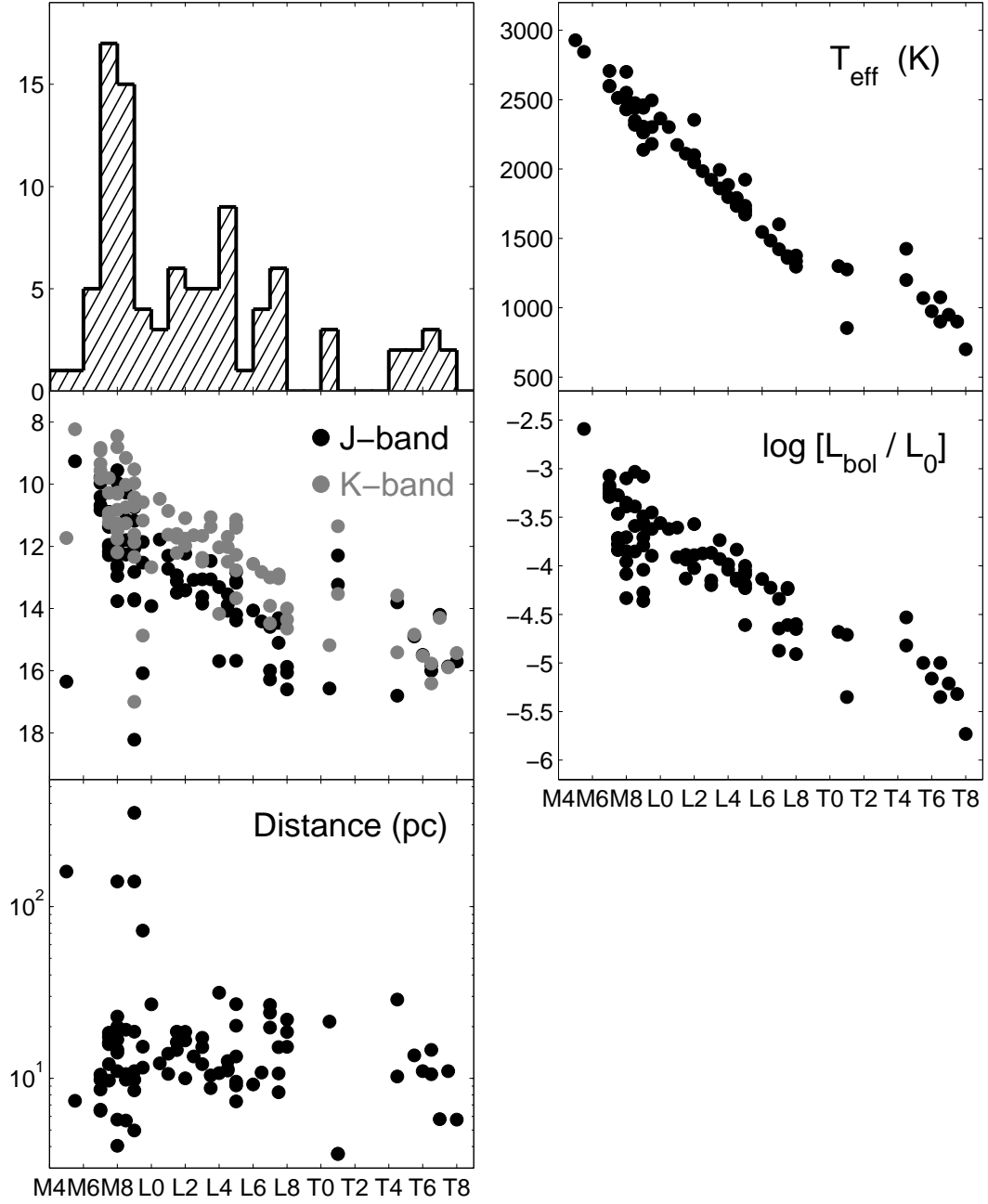


FIG. 1.— General properties of the survey sources, including spectral type, near-IR magnitudes, distances, effective temperatures, and bolometric luminosities.

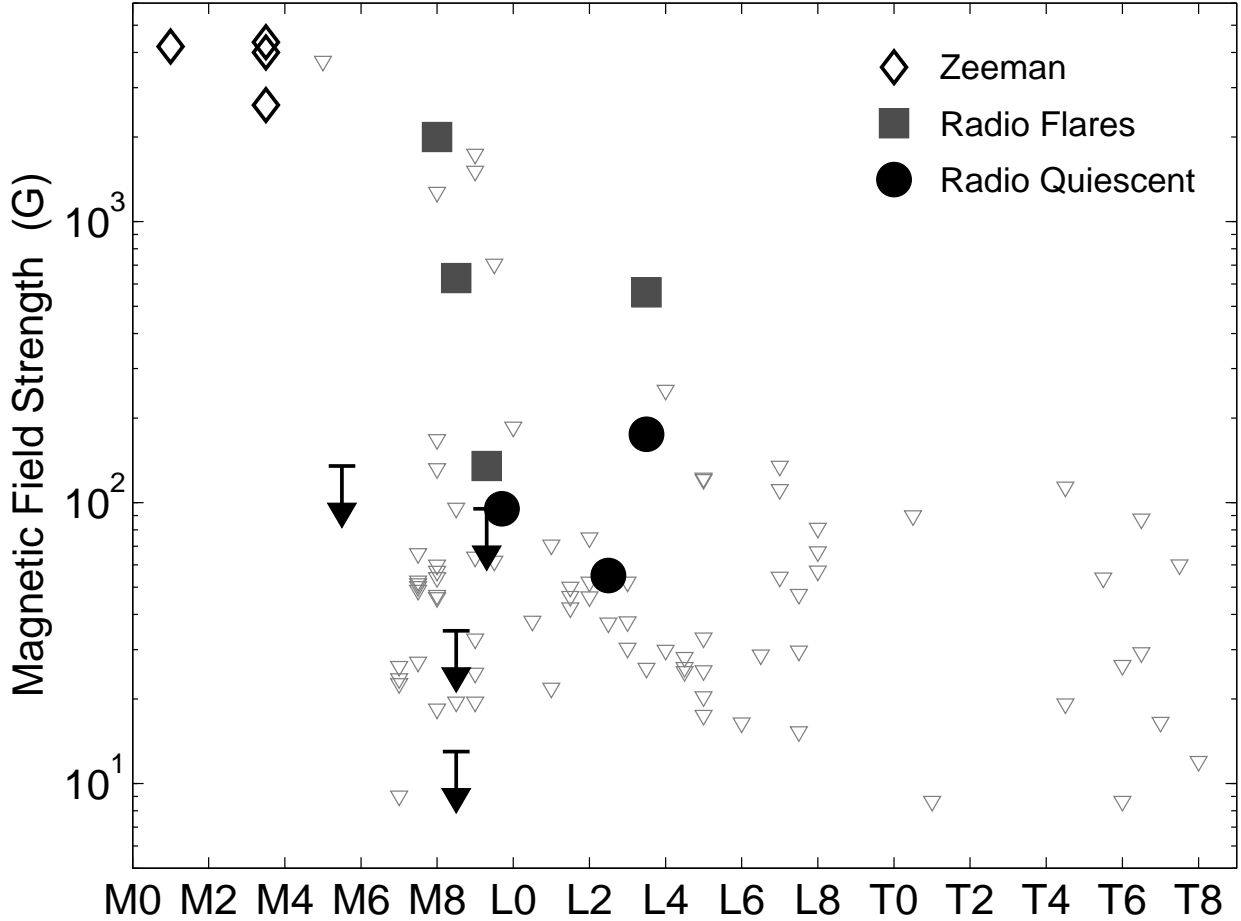


FIG. 2.— Magnetic field strengths and upper limits as inferred from the radio observations (quiescent: circles; flares: squares). Also shown are the values for early M dwarfs measured from Zeeman line broadening (Saar & Linsky 1985; Johns-Krull & Valenti 1996). We note that the surface field strength in the radio active dwarfs may up to an order of magnitude larger depending on the structure of the field and the height of the radio emitting region.

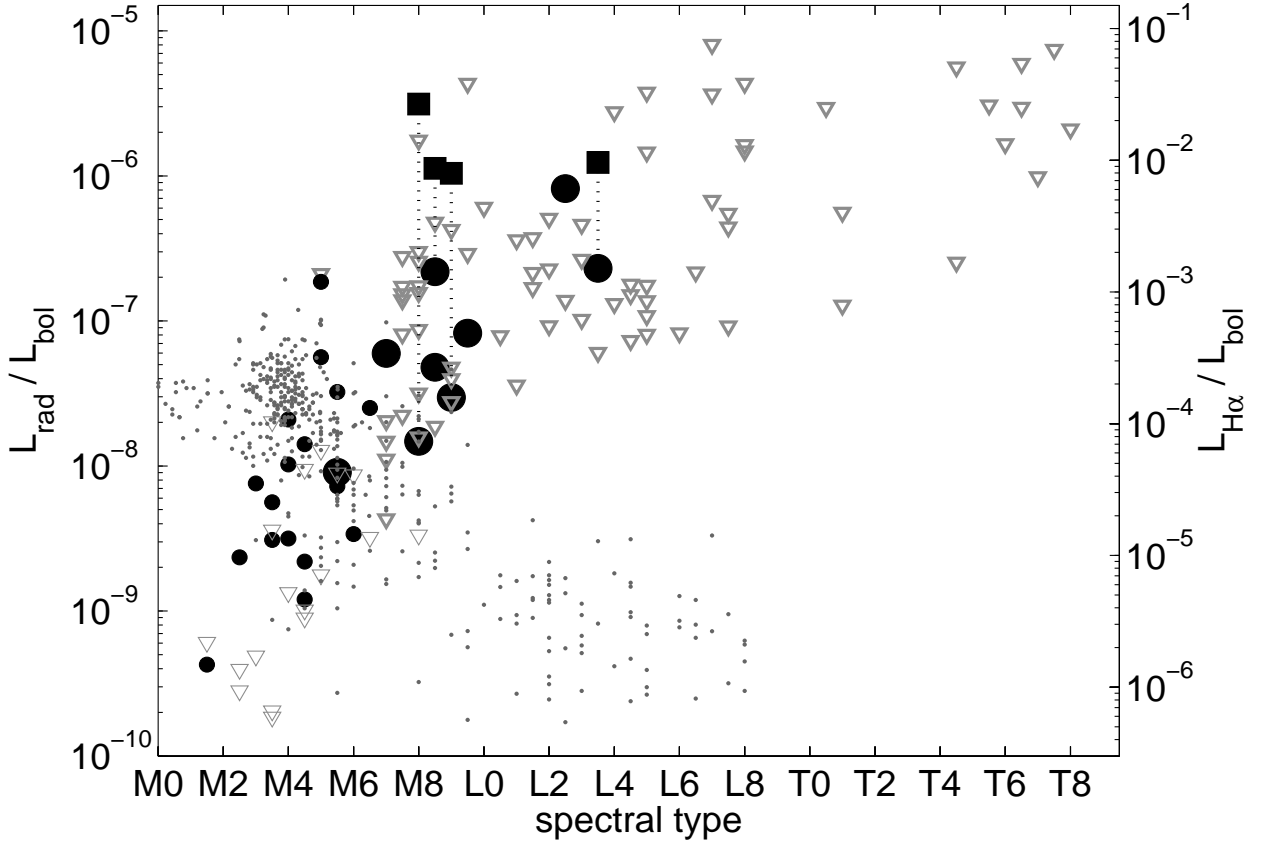


FIG. 3.— Radio and H $\alpha$  activity as a function of spectral type. Shown are flares (squares), quiescent emission (circles), and upper limits (triangles) in the radio; the H $\alpha$  observations are shown as gray dots. Note that the scale on the ordinate is different for the radio and H $\alpha$  observations. The trend of increased radio activity with later spectral type is evident, as is the overall drop in the fraction of detected objects. Unlike the radio emission, the H $\alpha$  emission drops beyond spectral type of about M7.

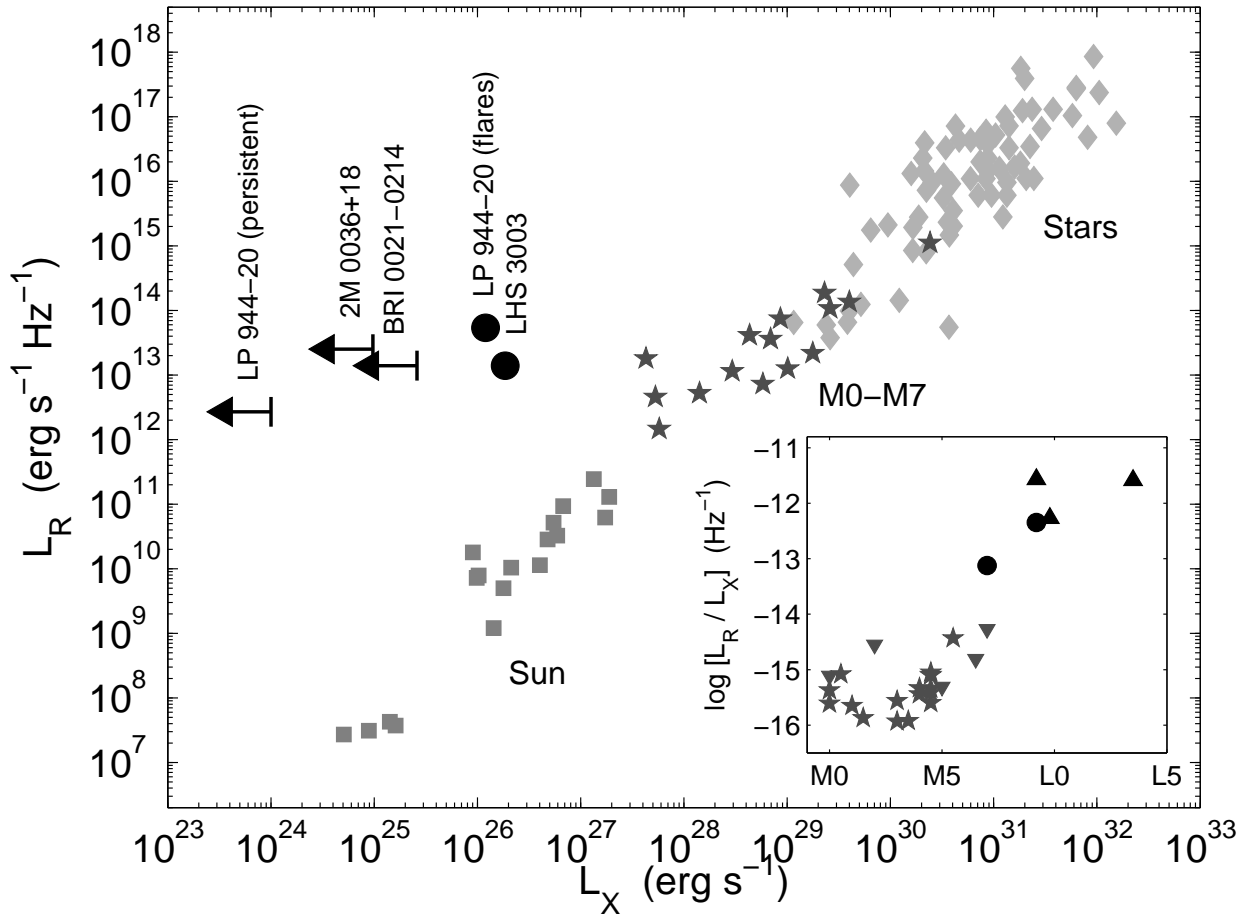


FIG. 4.— Radio vs. X-ray luminosity for stars exhibiting coronal activity. Data for late-M and L dwarfs are from Rutledge et al. (2000), Berger et al. (2001), Berger (2002), Berger et al. (2005), Burgasser & Putman (2005), while other data are taken from Güdel (2002) and references therein. Data points for the Sun include impulsive and gradual flares, as well as microflares. The strong correlation between  $L_R$  and  $L_X$  is evident, but begins to break down around spectral type M7 (see inset). The late-M and L dwarfs clearly violate the correlation and are over-luminous in the radio.